Chem Biol Drug Des 2010; **75:** 444–454

Research Article

© 2010 John Wiley & Sons A/S

doi: 10.1111/j.1747-0285.2010.00957.x

The Use of Biochemical and Biophysical Tools for Triage of High-Throughput Screening Hits – A Case Study with *Escherichia coli* Phosphopantetheine Adenylyltransferase

J. Richard Miller[1,2,*], Venkataraman Thanabal[1,3], Michael M. Melnick[1,4], Manjinder Lall[1,3], Charles Donovan[1], Ronald W. Sarver[1,5], Doh-Yeel Lee[1], Jeff Ohren[1,3] and Don Emerson[1,6]

[1]*Pfizer, Inc. Ann Arbor, MI 48105, USA*
[2]*Merck Research Laboratories Boston, MA 02115, USA*
[3]*Pfizer, Inc. Groton, CT 06340, USA*
[4]*Kalexsyn, Inc. Kalamazoo, MI 49008, USA*
[5]*Neogen, Inc. Lansing, MI 48912, USA*
[6]*Resonance Technologies, LLC Saline, MI 48176, USA*
**Corresponding author: James R. Miller, James.Miller2@merck.com*

High-throughput screening is utilized by pharmaceutical researchers and, increasingly, academic investigators to identify agents that act upon enzymes, receptors, and cellular processes. Screening hits include molecules that specifically bind the target and a greater number of non-specific compounds. It is necessary to 'triage' these hits to identify the subset worthy of further exploration. As part of our antibacterial drug discovery effort, we applied a suite of biochemical and biophysical tools to accelerate the triage process. We describe application of these tools to a series of 9-oxo-4,9-dihydropyrazolo[5,1-b]quinazoline-2-carboxylic acids (PQ) hits from a screen of *Escherichia coli* phosphopantetheine adenylyltransferase (PPAT). Initial confirmation of specific binding to phosphopantetheine adenylyltransferase was obtained using biochemical and biophysical tools, including a novel orthogonal assay, isothermal titration calorimetry, and saturation transfer difference NMR. To identify the phosphopantetheine adenylyltransferase sub-site bound by these inhibitors, two techniques were utilized: steady-state enzyme kinetics and a novel ^{19}F NMR method in which fluorine-containing fragments that bind the ATP and/or phosphopantetheine sites serve as competitive reporter probes. These data are consistent with PQs binding the ATP sub-site. In addition to identification of a series of PPAT inhibitors, the described hit triage process is broadly applicable to other enzyme targets in which milligram quantities of purified target protein are available.

Key words: 19F NMR, antibacterials, biophysics, calorimetry, phosphopantetheine, screening, triage

Received 28 October 2009, revised 19 January 2010 and accepted for publication 28 January 2010

Increasing bacterial resistance to antibiotics has driven efforts to find new agents that circumvent existing resistance mechanisms (1,2). Most efforts have focused on one or more of the following three approaches: (i) significant but incremental improvements of existing antibiotic classes; (ii) identification of novel chemical matter affecting an established antibacterial drug target (e.g. DNA topoisomerase, translation, *etc.*); or (iii) identification of inhibitors of novel drug targets. The sequencing of multiple bacterial genomes uncovered a wealth of potential targets that led many pharmaceutical and biotech companies to pursue this third option.

A commonly used method to identify small-molecule inhibitors of enzyme drug targets is *in vitro* high-throughput screening (HTS), in which collections of 10^5–10^6 individual compounds are tested for their ability to affect the activity of the target enzyme. Recently, public initiatives such as the Molecular Libraries Screening Centers Network (part of the NIH Roadmap for medical research) (3) and the efforts of institutions such as the McMaster University Screening lab (4), the Scripps Research Institute (5), St. Jude Children's Research Hospital (6), and many others have made HTS readily accessible to investigators outside of pharmaceutical companies.

In a typical HTS campaign against an enzyme target, an *in vitro* assay is developed with the purified protein(s), the assay is optimized and miniaturized, and is then used to assess the inhibitory effect of the molecules comprising a screening library. Depending on the target and assay, the output of such a HTS screen is typically a few hundred to few thousand compounds that reproducibly inhibit the assay signal. This list of 'hits' provides the substrate for further SAR (structure activity relationships) work. Unfortunately, with even the best-designed screening assay, the activity of many hits is not the result of a specific interaction with a desirable binding site on the target enzyme. Instead, the activity is attributable to non-specific effects such as the small-molecule hit interfering with the assay itself (e.g. quenching of the output signal, sequestering of the enzyme's substrate, insolubility of inhibitor in assay buffer, *etc.*). Alternately, some small molecules are promiscuous and

non-specifically inhibit the target through the formation of macromolecular aggregates (7). These aggregates may promote protein unfolding and/or sequester the protein molecules and thereby inactivate enzymes (8). In light of these and other undesirable mechanisms of inhibition, the first significant challenge of a drug discovery program emerging from HTS is to triage the list of hits to identify the set of molecules that specifically bind the target and are worthy of additional consideration.

Over the past 15 years, Pfizer, and several of its legacy organizations (Warner-Lambert and Pharmacia Corporation), have conducted more than 60 HTS campaigns against antibacterial targets. During this time, a number of biochemical and biophysical assays were developed and/or implemented that greatly accelerated HTS triage.

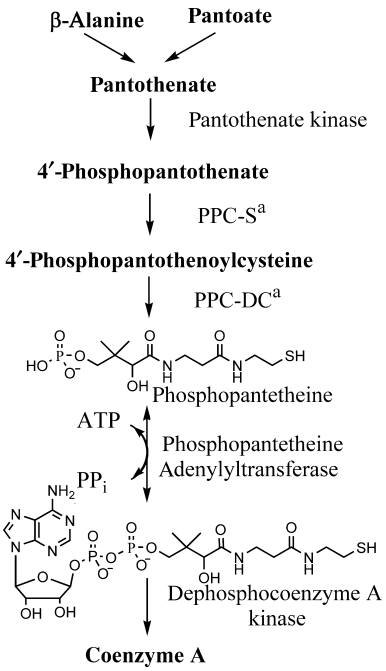

Figure 1: Coenzyme A (CoA) biosynthetic pathway. [a]PPC-S and PPC-DC are phosphopantothenoylcysteine synthetase and phosphopantothenoylcysteine decarboxylase, respectively. Both activities reside on a single polypeptide in *Escherichia coli*.

To demonstrate their practical application, we describe use of these tools within the context of an actual HTS triage effort around an essential enzyme target within the Coenzyme A (CoA) biosynthetic pathway, phosphopantetheine adenylyltransferase (PPAT). PPAT catalyzes the penultimate step of the CoA biosynthetic pathway; transfer of an AMP moiety from ATP to phosphopantetheine (PhP) yielding dephosphocoenzyme A (dPCoA, Figure 1) and inorganic pyrophosphate. Numerous crystal structures of PPAT with and without substrate ligands are available (9,10) and the kinetic mechanism of the *E. coli* enzyme has been investigated (11,12). Several other positive features led to the selection of PPAT as a target for high-throughput screening. These included a structurally attractive active site, a high degree of PPAT conservation across various bacterial species, distinct differences in active site residues between the human and bacterial enzymes, ready availability of large quantities of purified enzyme, and a straightforward enzyme-coupled kinetic assay (12).

In light of the appealing attributes of PPAT as an antibacterial drug discovery target, we performed a HTS of approximately one million compounds to identify PPAT inhibitors. Among the inhibitors identified, the most promising was a class of ATP-competitive 9-oxo-4, 9-dihydropyrazolo[5,1-b]quinazoline-2-carboxylic acids (PQs). In this manuscript, we describe their discovery, validation, and characterization using a combination of enzymological and biophysical triage tools (Figure 2). In addition, we describe a novel adaptation of fragment screening and ^{19}F-NMR to determine the PQ binding sub-site. Although applied to PPAT in this manuscript, the general triage strategy and the tools we utilize are broadly applicable to other enzyme-based drug discovery efforts.

Materials and Methods

Biochemical reagents

With the exception of phosphopantetheine and 7-methyl-8-thioguanosine (MESG), all biochemical reagents were from Sigma–Aldrich and were the highest purity available. Phosphopantetheine and MESG were sourced as described previously (12).

Production of Escherichia coli PPAT

PPAT from *E. coli* was prepared as described previously (12).

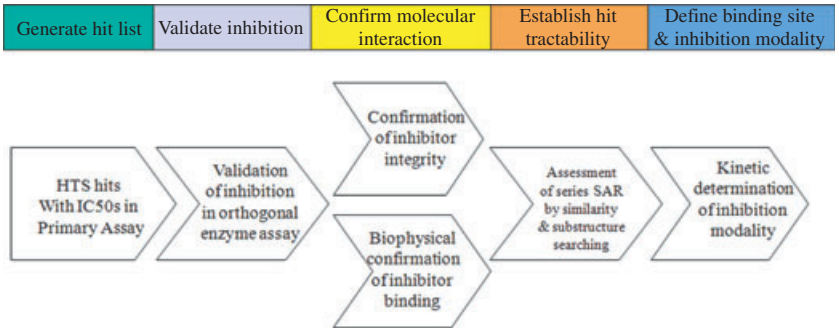

Figure 2: Sequential stages of an integrated high-throughput screening (HTS) hit triage utilizing biochemical and biophysical techniques.

Production of Enterococcus faecalis PPAT

The PPAT from *Enterococcus faecalis* strain V583 (ATCC# 700802D) was amplified from genomic DNA and cloned into the pET15b derivative pPW2 (Affinium Pharmaceuticals, Toronto, Ontario, Canada) and included both an N-terminal hexahistidine tag and a thrombin cleavage site. Expression and purification of this protein was identical to that previously described for *E. coli* PPAT (12). Assays of *E. faecalis* PPAT were performed as described for *E. coli* PPAT except that the ATP concentration was doubled to 40 μM because of the twofold higher $K_{m(ATP)}$ for the *E. faecalis* PPAT (data not shown).

High-throughput screening assay (forward-direction assay)

PPAT screening assays were performed in clear 384-well plates (Corning #3702) containing in each well either 1-μL DMSO (zero percent inhibition control), 1 μL of variable concentrations of test compounds solvated in DMSO, or 1 μL of a 100-μM solution of a dipeptide inhibitor of PPAT [Compound **8** from (13)] in DMSO, which serves as the fully inhibited control. To the entire plate, 20 μL of assay solution 1 (Table S1) was added using a multidrop dispenser (Titretek, Huntsville, AL, USA) and the plate was incubated for 5 min at room temperature. The plate was delivered to a second multidrop dispenser where 30 μL of solution 2 (Table S1) was added. The plate was then taken to a Spectramax plate reader (Molecular devices, Sunnyvale, CA, USA) and the change in absorbance at 360 nm was measured for 5 min. The rate of absorbance change was corrected for the background rate observed in the fully inhibited control. The corrected rate was then expressed as a percentage of the corrected rate observed in the uninhibited (DMSO only) control.

Reverse (ATP-generating) PPAT assay using firefly luciferase

The reverse assay was performed in polypropylene 96-well plates (Corning #3365) containing in each well either 1-μL DMSO (zero percent inhibition control), 1 μL of variable concentrations of test compounds solvated in DMSO, or 1 μL of a 100-μM solution of a dipeptide inhibitor of PPAT (Compound **8** from (13) in DMSO, which serves as the fully inhibited control. To the entire plate, 20 μL of assay solution 1 (Table S2) was added using a multidrop dispenser (Titretek) and the plate incubated for 5 min at room temperature. The plate was delivered to a second multidrop dispenser where 30 μL of solution 2 (Table S2) was added. The plate was then taken to a Beckman Multimek fitted with a 96-tip head. Aliquots (5 μL) of the reaction mix were removed at four equally spaced time intervals and transferred into a white 384-well plate (Corning #3705) containing 80 μL of solution 3 (Table S2) in each well. The plate was transferred to a Victor2 reader (Perkin Elmer, Wallac Turku, Finland) and the luminescence was immediately measured. The rate of change in luminescence was calculated from the time-point data. The rate was then expressed as a percentage of the rate observed in the uninhibited (DMSO only) control. Following reading of the plate, ATP was added to each well to give a final concentration of 20 μM and the luminescence was measured again. Wells that did not show a dramatic increase in luminescence were noted as interfering with the assay and were not used to fit inhibition data.

IC_{50} determinations

In both assays, inhibitor potency was assessed by duplicate 10-point titrations of inhibitor from 100 to 1 μM. Inhibition data were fit to the standard IC_{50} equation:

$$\frac{v_i}{v_0} = \frac{1}{1 + ([I]/IC_{50})^n} \quad (1)$$

where v_i is the reaction velocity at a given concentration of inhibitor [I], v_0 is the uninhibited velocity, and n is the Hill slope. IC_{50} assay replicates showed differences of ≤15%.

Isothermal titration calorimetry

The thermodynamics of PPAT ligand binding was determined using a VP-isothermal titration calorimetry (ITC) (Microcal, Northampton, MA, USA) as previously described (12) except that DMSO was added to the cell to give an equivalent concentration to that in the syringe when necessary. Ligands to be titrated were solvated at 30 mM in DMSO then diluted to 200–1000 μM in buffer (50-mM Tris, pH 8.0, 0.5-mM TCEP). For ITC studies conducted at pH 5–7, a 50-mM acetate buffer was utilized in place of Tris.

Steady-state kinetic inhibition assays

Assays to determine inhibition modality were performed using the same assay format as the forward-direction HTS assay described previously. Methodology was as described previously for product inhibition experiments (12) except that PQ inhibitors were utilized instead of PPAT reaction products. Steady-state kinetic and inhibition data were globally fit using the Enzyme Kinetics Module of Sigma Plot (Jandel Scientific, San Rafael, CA, USA), which allows comparison of fits to various inhibition schemes including competitive, non-competitive, uncompetitive, etc. The best model was selected based on the AIC.c [corrected Akaike information criterion, (14)], which allows direct comparison of models with different numbers of fitted parameters.

NMR methods

471 MHz $^{19}F(^{1}H$-decoupled) NMR spectra were collected at 25 °C on a Bruker DRX 500 MHz spectrometer equipped with a conventional 5-mm SEF probe optimized for ^{19}F detection. The spectra were collected using the CPMGC (PMG, Carr–Purcell–Meiboom–Gill) spin echo pulse sequence (15,16)with a t value of 20 ms and a total spin echo time of 320 ms. Data sets were the average of 128 scans.

Synthetic methods and spectral data

Synthetic procedures to produce analogues not previously described in the literature (17,18) are provided in the supplementary material.

Results

Identification/characterization of PQs by high-throughput screening

A previously described enzyme-coupled spectrophotometric phosphate detection assay (12) (Figure 3A) was adapted to a 384-well

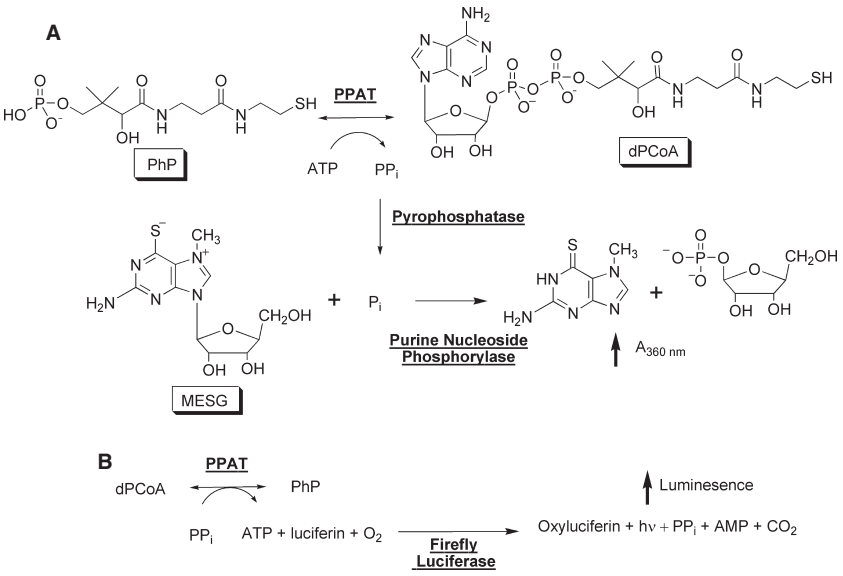

Figure 3: Enzyme-coupled phosphopantetheine adenylyltransferase (PPAT) assays with different methods of product detection. (A) Production of pyrophosphate in the forward-direction PPAT reaction is coupled to cleavage of a chromogenic nucleoside. (B) Production of ATP in the reverse-direction PPAT reaction is coupled to the generation of light by firefly luciferase.

high-throughput format to permit large-scale screening for PPAT inhibitors. The assay conditions were biased to identify ATP-competitive PPAT inhibitors and/or PhP-competitive inhibitors and are detailed in Table S1. The concentration of ATP used in the screen was 30 μM, well below the $K_{m(ATP)}$ of 220 μM (12). The concentration of PhP in the screen was held constant at 20 μM, fivefold higher than the K_m of PhP (12). Although this concentration of PhP was high enough to exclude very weak PhP-competitive inhibitors as hits, this was the minimum concentration of PhP needed to maintain a linear rate of product formation across the desired read-time of 5–10 min (data not shown).

Approximately, 1 million compounds were screened individually against PPAT. Several classes of inhibitors were identified, with the pyrazoloquinolones (PQs) shown in Table 1 being the most interesting. Members of this class of PQ inhibitors have previously been investigated for their antiallergic activity in animal models (17,18). The PQ series exhibited a range of *E. coli* PPAT IC_{50} values (Tables 1 and 2) suggesting the series possesses exploitable SAR. A plate-based nephelometer system (BMG LABTECH, Offenburg, Germany) was employed alongside these IC_{50} assays to ensure that IC_{50}s were well separated from the solubility limits of the compounds (data not shown).

PQs inhibit PPAT in a reverse (ATP-generating) PPAT assay

Hits identified by HTS can exhibit inhibition because of non-specific interference with the assay modality as described previously. To build confidence that the PQs are legitimate PPAT inhibitors, an alternative plate-based assay format was developed. *E. coli* PPAT has an equilibrium constant of approximately 1 (12), allowing use of the reverse reaction (ATP-generating) as a physiologically relevant alternative assay. In this assay, ATP is produced from dPCoA and inorganic pyrophosphate. We (12) and others (11) have coupled the PPAT reverse reaction to NADH production using hexokinase and glucose-6-phosphate dehydrogenase. PPAT turnover in this assay results in an increase in absorbance at 340 nm, but is considerably less sensitive than the HTS assay in Figure 3A (12). Furthermore, NADH formation is detected at a wavelength 20 nm lower than the primary assay and can be more susceptible to interference by inhibitor absorbance.

To avoid these issues and to provide another means to validate the PQ inhibitors, we developed a novel PPAT assay utilizing firefly luciferase to quantify the ATP generated by the PPAT reverse reaction (i.e. using dPCoA and inorganic pyrophosphate as substrates, Figure 3B). In the presence of ATP, firefly luciferase exhibits 'flash' kinetics with luminescence peaking then rapidly declining (19). However, when the luciferase inhibitor CoA is present, 'glow' kinetics are observed, where the peak luminescence is reduced but luminescence longevity is dramatically increased (19,20). This property is often employed in commercially available ATP-detection kits that advertise a 'stable' luminescence signal. These assays are configured such that the luminescence produced is proportional to the absolute ATP concentration of a quenched reaction mixture. This results in a discontinuous assay and therefore kinetic analysis of the PPAT reaction requires measurement of ATP concentrations at multiple time-points.

We utilized laboratory automation to capture four equally spaced time-points during the PPAT reverse reaction, enabling us to determine ATP concentrations and calculate the rate of ATP production. However, as the ATP concentrations of these samples needed to be analyzed after the samples were collected, a method to quench the PPAT reaction was required. Initially, we hypothesized that we could use CoA to both inhibit PPAT (12) and produce luciferase 'glow' kinetics. Inclusion of CoA at concentrations that fully inhibited the PPAT reverse reaction resulted in an unstable luminescence signal (data not shown) and was cost prohibitive for large-scale screening. We instead utilized high concentrations of PhP, which is a product inhibitor (12) of the PPAT reverse reaction, as a quenching agent. The final concentration of PhP utilized (200 μM) does not inhibit or activate luciferase (21) but does quench PPAT reactions sufficiently well that the luciferase signal (i.e. the ATP concentration) is stable for the 5–10 min required to read the luminescence of the assay

Table 1: *In vitro* inhibition of *Escherichia coli* and *Enterococcus faecalis* phosphopantetheine adenylyltransferase (PPAT) by 4- and 7-substituted pyrazoloquinolones

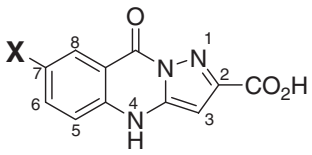

		Forward direction assay		Reverse direction assay
Compd	X	IC_{50} (μM) *E. coli* PPAT[a]	IC_{50} (μM) *E. faecalis* PPAT[a]	IC_{50} (μM) *E. coli* PPAT
6[b]	H	253	>167	>230
7[b]	CH_3	244	NT[e]	NT
8[b,d]	Cl	17	>75	NT
9[b]	F	103	>167	NT
10[c]	Br	6.2	209	22
11[c]	I	5.1	>137	11
12[b,d]	SCH3	13	>65	8.8
13[b]	$SOCH_3$	166	20	NT
14[b]	SO2CH3	92	NT	NT
15[b]	$SCH(CH_3)_2$	14	249	5.0
16[b]	$N(CH_3)_2$	49	157	7.1
17[b]	OCH3	>150	>167	NT
18[b]	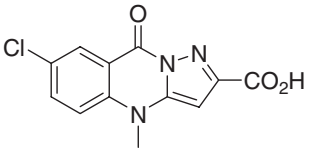	160	NT	NT

[a]Data with a greater than (>) sign indicate that PPAT inhibition was less than 50% at the highest tested or highest soluble concentration.
[b]Compound was present in the Pfizer compound library at the time of high-throughput screening (HTS).
[c]Compound was newly synthesized to expand series structure activity relationships (SAR).
[d]Compound was resynthesized to confirm activity.
[e]NT denotes compound was not tested.

plate. Also it is important to note that pyrophosphate, a PPAT reverse reaction substrate, is an inhibitor of luciferase luminescence production at concentrations utilized in the assay (19). As pyrophosphate was in large excess of the amount of ATP formed, the change in pyrophosphate concentration during the assay was negligible and thus the inhibitory effect on luciferase was uniform across all samples. Finally, a small amount of CoA was included to ensure 'glow' kinetics was maintained.

As some small-molecule inhibitors quench and/or inhibit luciferase luminescence and would therefore appear to inhibit the PPAT reaction, we also screened for this interference by adding a fixed amount of ATP (20 μM final concentration) to every well of the assay plate after reading the luciferase luminescence resulting from the PPAT reverse reaction. The amount of ATP added is in excess to that generated in the PPAT reaction, but well below that which would saturate the luciferase enzyme (data not shown). Compound-specific quenching was readily apparent as these wells did not show a dramatic increase in luminescence upon ATP addition.

The PQs inhibited PPAT in this reverse reaction assay (Tables 1 and 2) and did not inhibit luciferase (data not shown), indicating that their inhibition was not because of interference with the primary assay. For most analogues tested in the reverse PPAT assay (excluding compound **16**), the rank order potencies corresponded well between the two assays. However, because of the differences in the ratios of substrate concentrations to the substrate K_m values, there is no expectation that the absolute IC_{50} values be identical between the two assays.

Selectivity and specificity of the PQ inhibitors

Given our interest in discovering selective broad-spectrum antibacterial agents, it was important to determine the potency of the PQ inhibitors against a PPAT from a divergent yet medically relevant pathogen. As the primary screen was performed against the PPAT from the Gram-negative *E. coli*, we selected the *E. faecalis* PPAT as a reasonable representative of Gram-positive PPAT enzymes. The *E. faecalis* enzyme displays only 44% protein sequence identity to the *E. coli* PPAT. Interestingly, with the exception of **13** and **16**, all compounds were inactive versus *E. faecalis* PPAT (Tables 1 and 2). Selectivity against the human PPAT is also critically important, and none of the PQs tested inhibited the human PPAT at concentrations up to 100 μM (data not shown).

Newly resynthesized PQs show PPAT inhibitory activity

Although considerable effort is made to ensure the accurate identity and structural integrity of compounds in screening files, it is

Table 2: *In Vitro* inhibition of *Escherichia coli* and *Enterococcus faecalis* phosphopantetheine adenylyltransferase (PPAT) by 3- and 6-substituted pyrazoloquinolones

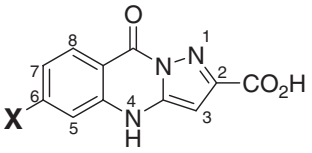

Compound	X	Forward direction assay		Reverse direction assay
		IC_{50} (μM) *E. coli* PPAT[a]	IC_{50} (μM) *E. faecalis* PPAT[a]	IC_{50} (μM) *E. coli* PPAT
6[b]	H	253	>167	>230
19[c]	CH_3	15	>167	NT[d]
20[c]	CF_3	54	>167	200
21[b]	NH_2	121	100	NT
22[b]	Br	124	>167	>125
23[b]	Cl	49	212	93
24[b]	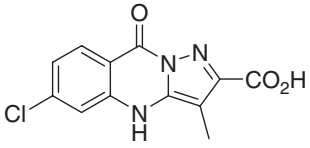	106	>167	NT

[a]Data with a greater than (>) sign indicate that phosphopantetheine adenylyltransferase (PPAT) inhibition was less than 50% at the highest tested or highest soluble concentration.
[b]Compound was present in the Pfizer compound library at the time of high-throughput screening (HTS).
[c]Compound was newly synthesized to expand series structure activity relationships (SAR).
[d]NT denotes compound was not tested.

not uncommon for structures to be incorrectly assigned or for samples to have partially degraded – particularly if they are many years old (e.g. the PQ analogues in our file were approximately 20 years old). Additionally, contaminants from the synthetic route (i.e. purification resins, heavy metals, etc.) can be present. In each of these cases, the contaminants could be the actual inhibitory agent. To rule this out, it is critical to resynthesize representative or close-in analogues using modern and preferably orthogonal synthetic schemes that minimize or eliminate these potential contaminants.

The chemistry reported by Sircar (17,18) and shown in Figure 4 was utilized to prepare additional analogues. The route used substituted anthranilic acids **1** as the starting material. Conversion of **1** to isatoic anhydride **2** was readily accomplished with triphosgene in THF. Reaction of **2** with excess hydrazine hydrate produced hydrazide **3** that could be reacted with **4** followed by base hydrolysis to yield the final PQs **5** in acceptable yield. Several PQ analogues were resynthesized as described in Figure 4 and were observed to inhibit PPAT in both the forward and reverse-direction assays (Tables 1 and 2).

SAR of PQ inhibitors

Although a number of PQ analogues were present in the Pfizer corporate collection, we wished to further explore the SAR of this series and additional analogues were synthesized using the route described in Figure 4. Table 1 summarizes the SAR for analogues that were varied in the 7- and 4-positions. When X is hydrogen, the IC_{50} against *E. coli* PPAT was found to be 253 μM. Interestingly, the activity improved by a factor of 50-fold when either the proton, Me or F groups, which were essentially equipotent, were replaced with either bromine or iodine, with the 7-iodo displaying an IC_{50} against *E. coli* PPAT of 5 μM. This suggests that substituents in the 7-position may be interacting with a carbonyl oxygen in the PQ binding pocket through an induced dipole effect (22,23). Replacement of the proton with a SMe group also resulted in an approximately 20-fold increase in activity over the unsubstituted analogue and this was maintained when the methyl was replaced with an isopropyl group. However, replacement of the SMe group with OMe or oxidation of SMe produced an approximately 10-fold loss in activity. This finding also lends credence to the induced dipole interaction hypothesis. Replacing the

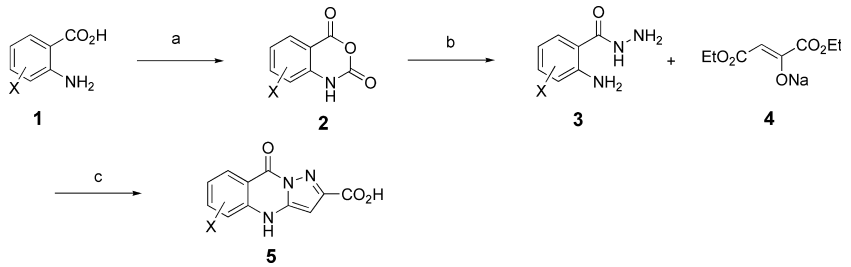

Figure 4: Reagents and conditions for synthesis of pyrazoloquinolones (PQs): (a) triphosgene, tetrahydrofuran at room temperature; (b) excess hydrazine hydrate; (c) H_2O, reflux, followed by Na_2CO_3.

proton with a dimethylamine in the 7-position was moderately tolerated. Replacement of the proton at the 4-position of the 7-chloro analogue resulted in a nearly 10-fold decrease in potency, indicating the requirement for a hydrogen bond donor at this position.

Table 2 summarizes the SAR for analogues that were varied in the 6- and 3-positions. In general, adding moderate bulk in the 6-position, e.g. Me or CF_3 resulted in improved potency over the unsubstituted PQs. The 6-position seems to reside in a somewhat smaller and more hydrophobic pocket as opposed to the 7-position. For example, the Br and amine substituents were essentially equipotent and possessed IC_{50} values that were about half that of the smaller Cl or CF_3 groups. Unfortunately, despite exhaustive efforts, we were not able to determine a co-crystal structure or even generate a plausible docking model for the PQs that were able to explain all the SAR. It is likely that the PQs bind toward the extremity of the ATP binding site as tested compounds were competitive with ATP but not with AMP (data not shown), but a conclusive evaluation of the PQ binding site in PPAT will have to wait for additional structural studies.

PPAT binds PQs

When newly resynthesized hits show inhibition in the primary and orthogonal assay(s), there is increased confidence in their validity. However, these data do not demonstrate specific interaction with the target protein. To provide evidence that PQs directly interact with PPAT, we utilized ITC to examine the interaction of compound **12**. In the same buffer and pH conditions used in the enzyme assays, **12** bound the apo-enzyme with a dissociation constant (K_d) of 24.4 ± 0.7 μM (Figure 5), similar to the IC_{50} in the enzyme assays (Table 1). Binding to PPAT was enthalpically driven (−5.2 ± 0.1 kcal/mol) and exhibited 1:1 binding stoichiometry, similar to ATP, PhP, and dPCoA (12).

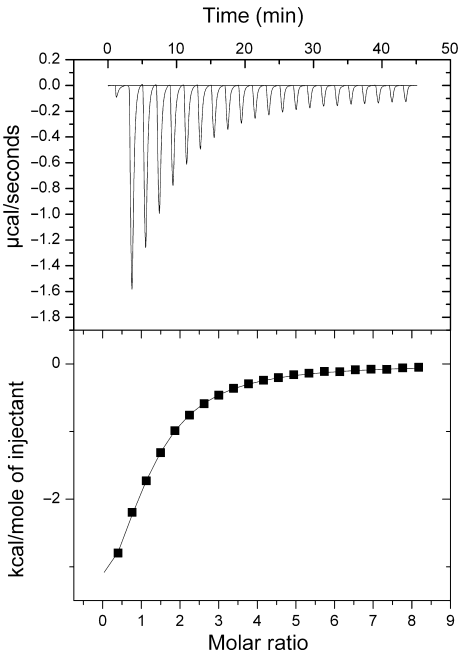

Figure 5: Binding of **12** to *Escherichia coli* phosphopantetheine adenylyltransferase (PPAT) as monitored by isothermal titration calorimetry (ITC). The top panel shows the change in calorimeter power required to maintain constant temperature after each injection of **12**. The bottom panel shows the integrated heats of binding corrected for heats of dilution, and the solid line is the best fit of the data to a single-site binding model.

PQs are ATP competitive inhibitors of PPAT

Previously discussed evidence argues that PQs are specific inhibitors of PPAT but do not provide information about the modality of inhibition. Therefore, PPAT inhibition by PQs was examined by steady-state kinetics using the HTS-format assay (Figure 3A). When increasing concentrations of PQ inhibitor **11** were tested against PPAT at variable concentrations of one substrate and fixed, saturating concentrations of the other substrate, **11** was competitive with ATP (K_i of 5.1 ± 0.6 μM) as shown in Figure 6A. At saturating concentrations of ATP, **11** had no significant effect on the rate of PPAT turnover across a wide range of phosphopantetheine concentrations (Figure 6B). The K_i value of **11** determined from this study was comparable to other assessments of binding potency (Table 1).

Use of trifluoromethyl-containing fragments to probe inhibitor binding sites

As part of our efforts to identify novel PPAT inhibitors, we also performed a saturation transfer difference nuclear magnetic resonance spectroscopy (STD-NMR) screen of a small library of low molecular weight fragments (general properties of the fragment library are discussed in the supplementary material). This screen identified a number of molecules that interacted with PPAT. None of these exhibited sufficient chemical attractiveness/ligand efficiency to pursue with additional medicinal chemistry resources (data not shown). However, several hits contained trifluoromethyl substituents and their binding to PPAT can be readily monitored by ^{19}F NMR (see below).

Previous work by other authors has shown that weakly binding fluorine-containing molecules can serve as 'spy' probes that can be competed off by a more tightly bound ligand (24) and that fluorine-containing fragment libraries have potential for fragment-based drug discovery (25).The use of ^{19}F NMR to monitor ligand–protein interactions provides simplified NMR spectra without interference from the proton signals (24,26) We sought to take advantage of the favourable NMR properties of fluorine to validate the binding of the PQ inhibitors to PPAT.

The fluorine-containing probes **25** and **26** (Figure 7) identified in the STD-NMR fragment screen interact with PPAT as gauged by ^{19}F NMR (Figure 8). Both compounds have PPAT IC_{50}s greater than 100 μM in all assays (data not shown). Despite their weak affinity, a CPMG spin echo based pulse sequence showed that they are displaced upon addition of ATP and/or phosphopantetheine, respectively (Figure 8).

We have utilized these weakly binding CF_3-containing fragments as reporter probes to classify compound **10** as an ATP site binder. Figure 8A shows the ^{19}F (^1H decoupled) spectra of **25** and **26**. The

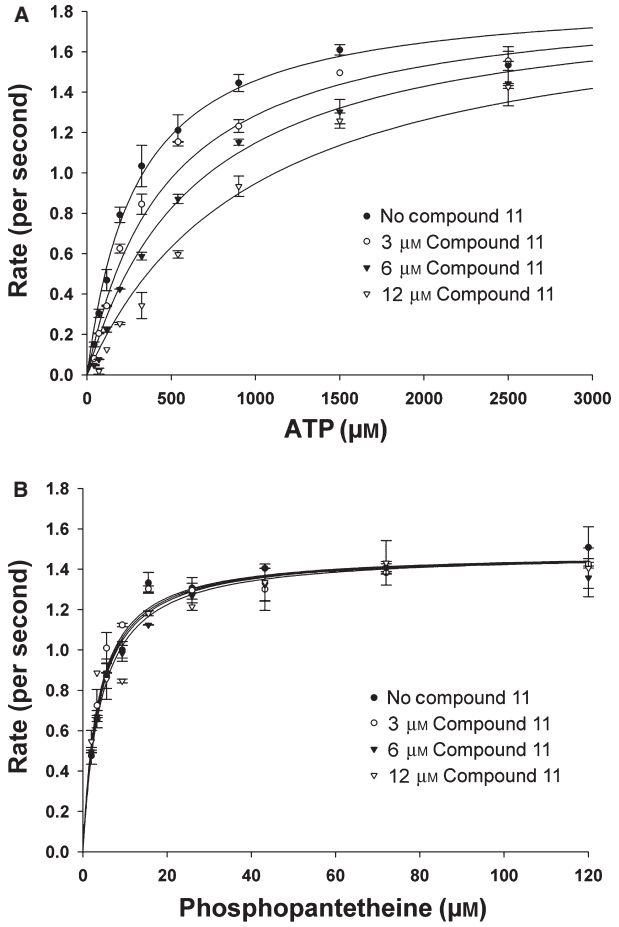

Figure 6: Steady-state kinetics of phosphopantetheine adenylyltransferase (PPAT) inhibition by **11**. The assay shown in Figure 3A was used to determine the rate of PPAT turnover at variable concentrations of substrate and inhibitor. (A) The concentration of ATP was varied at a constant saturating concentration of PhP (200 μM). The rates of PPAT turnover were then measured at the following concentrations of compound **11**: 0 μM (filled circles), 3 μM (unfilled circles), 6 μM (filled triangles), 12 μM (unfilled triangles). (B) PPAT rates with variable concentrations of PhP and saturating concentrations of ATP (2 mM). Concentrations of **11** are as shown in panel A.

two signals at −76.56 and −76.08 correspond to the CF_3 groups of fragments **25** and **26,** respectively. Upon addition of PPAT, these ^{19}F signals disappear because of the faster relaxation of the CF_3 group that occurs upon binding to PPAT (Figure 8B). Addition of ATP to a mixture of PPAT and compounds **25** and **26** displaces only compound **25** as evidenced by the selective appearance of the ^{19}F signal at −76.56 ppm (Figure 8C). Note that the ^{19}F peak of compound **25** does not return to its original intensity. This may indicate that **25** weakly binds PPAT at an additional site that is not affected by addition of substrate. Addition of PhP to the mixture of PPAT, **25**, and **26** displaces both fragments as evidenced by the appearance of both the ^{19}F signals (Figure 8D). The ATP sub-site specific signal at −76.56 again exhibits only partial intensity recovery indicating that **25** is not fully competed out by PhP, whereas **26** is. It

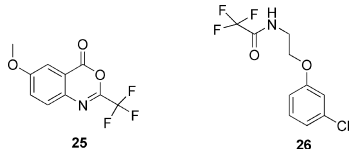

Figure 7: Active site probe fragments for use in phosphopantetheine adenylyltransferase (PPAT) ^{19}F NMR competition experiments.

is possible that **25** binds PPAT in a position that overlaps both the ATP and the PhP pocket. Figure 9 demonstrates using these tools to classify the PQ hits. ^{19}F spectra of both ATP and PhP reporter fragments alone and in the presence of PPAT are shown in Figures 9A and 9B respectively. Addition of **10** to a solution containing PPAT, **25,** and **26** selectively displaces only the ATP probe **25** as evidenced by the appearance of its ^{19}F signal at −76.56 ppm (Figure 9C). As observed above, the peak height of **25** does not fully return upon addition of **10,** providing additional evidence for a second non-active site interaction of **25** with PPAT.

These data (in conjunction with the steady-state inhibition kinetics described previously) strongly suggest that the PQs interact with the ATP pocket of PPAT. However, it is possible that the PQs may act in an allosteric fashion; binding outside the active site and remotely affecting the interaction of ATP and/or fragment **25**.

PQ binding affinity is pH dependent and implications for Structure Based Drug Design (SBDD)

Despite considerable effort, we were unable to obtain co-structures of PQ inhibitors with PPAT. The conditions under which PPAT readily crystallizes are acidic (pH <6), whereas our assay conditions are at pH 8.0. To determine whether this significant difference in pH could explain our inability to obtain co-structures, we used ITC to measure the binding affinity of a representative PQ as a function of pH (Table 3). Although changes in affinity could be as a result of changes in the ionization state of the inhibitor or the protein, PQ **12** exhibited no detectable binding at pH 6.0. Similarly, the potent PPAT inhibitor CoA exhibited a 100-fold weaker binding potency at pH 6.0 versus that at pH 8.0 as measured by ITC. Although significantly weaker at the lower pH, CoA binds with sufficient affinity to obtain a PPAT:CoA co-crystal structure (10).

Conclusions and Future Directions

The data and examples we provide demonstrate tools and techniques that can be used to increase confidence in the validity of hits from HTS campaigns. The essential characteristics of a tractable screening hit are: (i) does not interfere with the primary assay; (ii) structurally intact and retains activity upon resynthesis; (iii) close-in analogues possess a range of potency indicating definable SAR; (iv) specifically interacts with the target enzyme at a discrete site. Our general approach to establishing these criteria is depicted in Figure 2 and the quantitative outcome of applying these

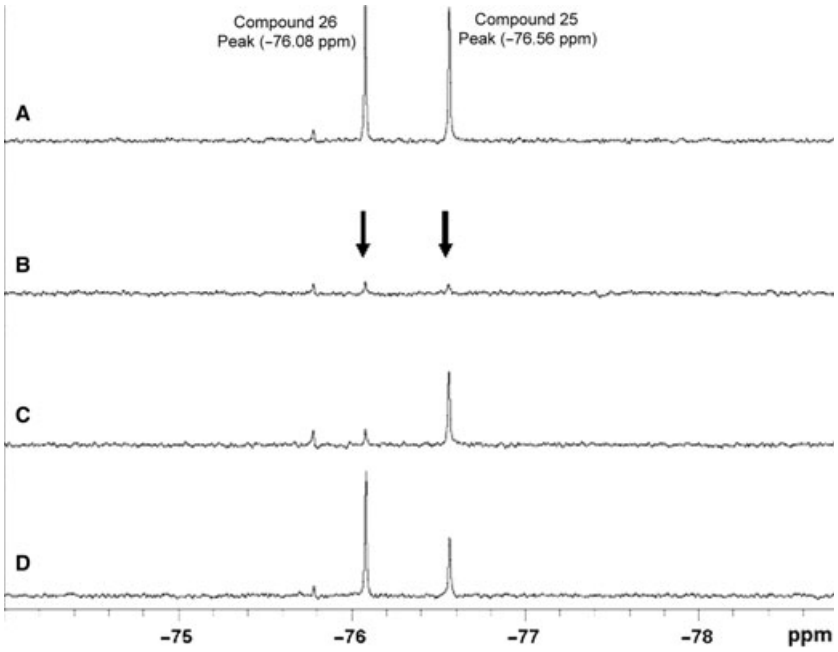

Figure 8: ^{19}F NMR spectra of fluorine-containing fragments with and without addition of phosphopantetheine adenylyltransferase (PPAT) and/or PPAT substrates. (A) 471 MHz $^{19}F(^{1}H$-decoupled) NMR spectrum of 100 μM each of **25** and **26** in 10-mM HEPES-*d*18, pH 8.0, 25 °C. (B) Addition of 4-μM (final concentration) PPAT causes loss of the indicated peaks because of the fast relaxation that results from PPAT binding. (C) Addition of 400-μM ATP to the sample in (B) selectively displaces the fragment **25** as evidenced by the appearance of the signal at −76.56 ppm. (D) Addition of 200-μM PhP to the sample in (B) displacing both **25** and **26** as evidenced by the appearance of signals at −76.08 and −76.56 ppm. All the spectra were collected using the CPMG spin echo sequence with a total spin of 320 ms. ^{19}F chemical shifts were referenced with respect to trifluoroethanol.

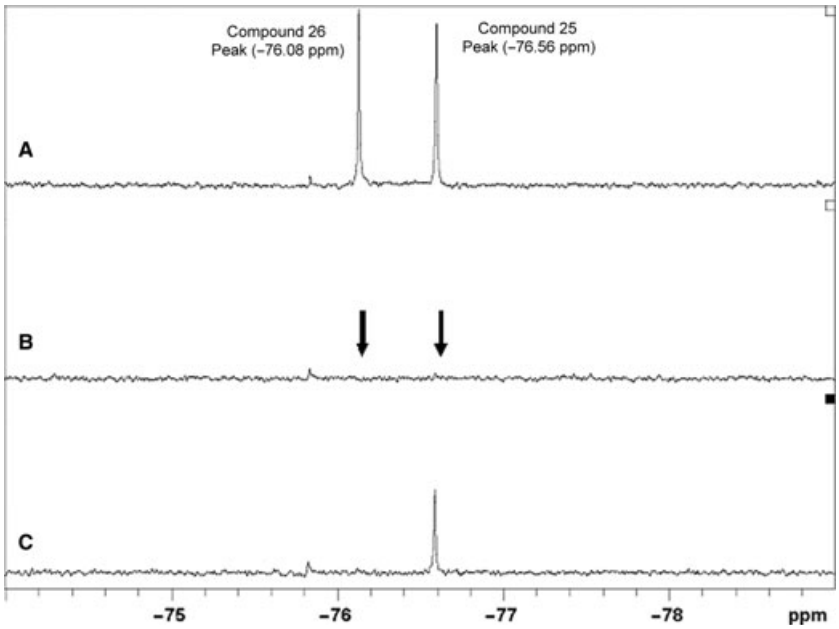

Figure 9: ^{19}F NMR spectra of fluorine-containing fragments with and without addition of phosphopantetheine adenylyltransferase (PPAT) and/or pyrazoloquinolone (PQ) inhibitors. (A) 471 MHz $^{19}F(^{1}H$-decoupled) NMR spectrum of 100 μM each of **25** and **26** in 10-mM Hepes-d18, pH 8.0, 25 °C. (B) Addition of 4-μM PPAT causes the peaks designated by arrows to disappear, due to fast relaxation as a result of binding to PPAT. (C) Addition of 100 μM of **10** to the sample in (B). Compound **10** selectively competes with the ATP probe fragment **25** as evidenced by the appearance of the signal at −76.56 ppm.

Table 3: Dependence of CoA and pyrazoloquinolone (PQ) binding affinity on pH as determined by isothermal titration calorimetry

	K_d (μM)	
pH	Coenzyme A (CoA)	Compound **12**
8.0	0.09	24
7.0	4.6	22
6.0	10	>200
5.0	72	>200

approaches to the PPAT screening hits is shown in Figure 10. Although elimination of the majority of hits occurred in the early stages of triage (primary and orthogonal/secondary assays), the use of biophysical approaches such as STD-NMR and isothermal titration calorimetry eliminated all but a few unique compounds (often referred to as singletons) or series of related compounds that required more intensive enzymological characterization and synthetic follow-up.

We have used a variety of tools including a novel application of ^{19}F NMR and fragment screening to establish the previously described four validation criteria for the PQ series of PPAT inhibitors. We chose to present kinetic, thermodynamic, and NMR binding data for three different PQs rather than data for the most potent compound

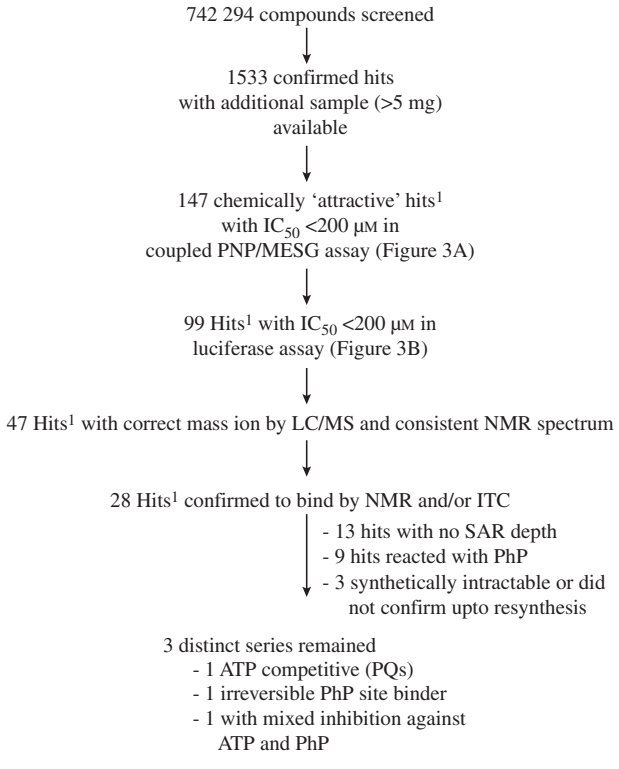

[1]In the noted cases, the term hits counts clusters of structurally related compounds (such as the pyrazoloquinolones) as a single hit

Figure 10: Quantitative detail of the phosphopantetheine adenylyltransferase (PPAT) high-throughput screening (HTS) triage process.

to reinforce the importance of collecting data for several members of a high-priority compound series rather than just the most potent analogue. Although we have presented these studies with different analogues, all of the featured analogues exhibited favourable binding data in each test (data not shown).

Often, practical considerations such as limited availability of analogues, poor inhibitor solubility, or incompatibility of a target with one or more tools/assays preclude confirming all validation criteria for each series of hits. When a full suite of assay data is not available for every compound of interest, the data in hand can be used to 'bin' hit series (or singletons) into high-, medium-, or low-priority groups for follow-up. Other project-specific considerations, such as selectivity and attractive physicochemical properties are also important and should receive due consideration.

The PQ series of PPAT inhibitors meet the four points mentioned previously and are therefore suitable for further exploration by synthetic medicinal chemistry. They possess several attractive physicochemical and pharmacokinetic properties (data not shown) such as a high aqueous solubility, low LogD (-2), stability in the presence of human liver microsomes, no significant cytochrome P-450 inhibition, and do not inhibit the PPAT reaction of the bi-functional human CoA synthase. This selectivity against the human ortholog is not surprising given the low conservation between the two genes (data not shown). The PQs were not observed to inhibit other ATP-binding proteins such as protein kinases based on their failure to 'hit' these targets in numerous previous HTS campaigns (data not shown). Despite these positive features, the compounds exhibit a dramatically pH-dependent binding profile and lack co-crystal structure(s) to guide medicinal chemistry efforts. They also do not possess antibacterial activity, likely because of their modest potencies against PPAT or their inability to penetrate the bacterial cell wall. This sort of 'mixed' profile for a compound series (i.e. some supporting data and some inconclusive data) is common for hits emerging from HTS and decisions must be made about the risk of proceeding with these assets and liabilities in place.

References

1. Payne D.J., Gwynn M.N., Holmes D.J., Pompliano D.L. (2007) Drugs for bad bugs: confronting the challenges of antibacterial discovery. Nat Rev Drug Discov;6:29–40.
2. Silver L.L. (2005) A retrospective on the failures and successes of antibacterial drug discovery. IDrugs;8:651–655.
3. Austin C.P., Brady L.S., Insel T.R., Collins F.S. (2004) NIH Molecular Libraries Initiative. Science;306:1138–1139.
4. Brown E.D. (2003) Screening in academe: a perspective on implementation of university-based small molecule screening. J Biomol Screen;8:377–379.
5. Sheppard T.L. (2007) Scripps Florida. Nat Chem Biol;3:451.
6. Chen T., Guy R.K. (2008) High-Throughput Screening and Drug Discovery at St. Jude Children's Research Hospital. Cell Notes;22:3–4.
7. McGovern S.L., Caselli E., Grigorieff N., Shoichet B.K. (2002) A common mechanism underlying promiscuous inhibitors from virtual and high-throughput screening. J Med Chem;45:1712–1722.

8. Coan K.E., Maltby D.A., Burlingame A.L., Shoichet B.K. (2009) Promiscuous aggregate-based inhibitors promote enzyme unfolding. J Med Chem;52:2067–2075.
9. Izard T. (2002) The crystal structures of phosphopantetheine adenylyltransferase with bound substrates reveal the enzyme's catalytic mechanism. J Mol Biol;315:487–495.
10. Izard T. (2003) A novel adenylate binding site confers phosphopantetheine adenylyltransferase interactions with coenzyme A. J Bacteriol;185:4074–4080.
11. Geerlof A., Lewendon A., Shaw W.V. (1999) Purification and characterization of phosphopantetheine adenylyltransferase from Escherichia coli. J Biol Chem;274:27105–27111.
12. Miller J.R., Ohren J., Sarver R.W., Mueller W.T., de Dreu P., Case H. and Venkataraman Thanabal (2007) Phosphopantetheine adenylyltransferase from Escherichia coli: investigation of the kinetic mechanism and role in regulation of coenzyme A biosynthesis. J Bacteriol;189:8196–8205.
13. Zhao L., Allanson N.M., Thomson S.P., Maclean J.K., Barker J.J., Primrose W.U. *et al.* (2003) Inhibitors of phosphopantetheine adenylyltransferase. Eur J Med Chem;38:345–349.
14. Akaike H. (1976) An information criterion (AIC). Math Sci;14:5–9.
15. Carr H.Y., Purcell E.M. (1954) Effects of Diffusion on Free Precession in Nuclear Magnetic Resonance Experiments. Phys Rev;94:630–638.
16. Meiboom S., Gill D. (1958) Modified spin-echo method for measuring spin-relaxation rates. Rev Sci Intrum;29:688–691.
17. Sircar J.C., Capiris T., Kesten S.J., Herzig D.J. (1981) Pyrazolo[5,1-b]quinazolin-9-ones: a new series of antiallergic agents. J Med Chem;24:735–742.
18. Sircar J.C., Capiris T., Kesten S.J. (1981) Reactions of 2H-3,1-Benzoxazine-2,4-(1H)dione (Isatoic Anhydride) with Anions of 1,4-Dihydro-5H-Pyrazol-5-ones: Synthesis of Pyrazolo [5,1-b]quinazolin-9-ones. J Heterocycl Chem;18:117–121.
19. Ford S.R., Chenault K.H., Bunton L.S., Hampton G.J., McCarthy J., Hall M.S., Pangburn S.J., Buck L.M., Leach F.R. (1996) Use of firefly luciferase for ATP measurement: other nucleotides enhance turnover. J Biolumin Chemilumin;11:149–167.
20. Airth R.L., Rhodes W.C., Mc Elroy W.D. (1958) The function of coenzyme A in luminescence. Biochim Biophys Acta;27:519–532.
21. Ford S.R., Buck L.M., Leach F.R. (1995) Does the sulfhydryl or the adenine moiety of CoA enhance firefly luciferase activity? Biochim Biophys Acta;1252:180–184.
22. Voth A.R., Khuu P., Oishi K., Ho P.S. (2009) Halogen bonds as orthogonal molecular interactions to hydrogen bonds. Nat Chem;1:74–79.
23. Lu Y., Shi T., Wang Y., Yang H., Yan X., Luo X. *et al.* (2009) Halogen Bondingî-A Novel Interaction for Rational Drug Design? J Med Chem;52:2854–2862.
24. Dalvit C., Fagerness P.E., Hadden D.T.A., Sarver R.W., Stockman B.J. (2003) Fluorine-NMR experiments for high-throughput screening: theoretical aspects, practical considerations, and range of applicability. J Am Chem Soc;125:7696–7703.
25. Vulpetti A., Hommel U., Landrum G., Lewis R., Dalvit C. (2009) Design and NMR-Based Screening of LEF, a Library of Chemical Fragments with Different Local Environment of Fluorine. J Am Chem Soc;131:12949–12959.
26. Dalvit C. (2007) Ligand- and substrate-based 19F NMR screening: principles and applications to drug discovery. Prog Nucl Magn Reson Spectrosc;51:243–271.

Supporting Information

Additional supporting information may be found in the online version of this article.

Data S1. Synthesis and analytical assessment of compounds.

Table S1. Composition of solutions used in the forward direction PPAT HTS assay.

Table S2. Composition of solutions used in the reverse-direction PPAT assay.

Please note: Wiley-Blackwell is not responsible for the content or functionality of any supporting materials supplied by the authors. Any queries (other than missing material) should be directed to the corresponding author for the article.